J. Membrane Biol. 144, 21–30 (1995)

The Journal of
Membrane
Biology

The Chloride Concentration in the Lateral Intercellular Spaces of MDCK Cell Monolayers

P. Xia, B.-E. Persson*, K. R. Spring

Laboratory of Kidney and Electrolyte Metabolism, National Heart, Lung, and Blood Institute, National Institutes of Health, Bethesda, Maryland 20892-1598

Received: 23 August 1994/Revised: 10 November 1994

Abstract. We measured the Cl concentration of the lateral intercellular spaces (LIS) of MDCK cell monolayers, grown on glass coverslips, by video fluorescence microscopy. Monolayers were perfused at 37°C either with HEPES-buffered solutions containing 137 mM Cl or bicarbonate/CO_2-buffered solutions containing 127 mM Cl. A mixture of two fluorescent dyes conjugated to dextrans (MW 10,000) was microinjected into domes and allowed to diffuse into the nearby LIS. The Cl-sensitive dye, ABQ-dextran, was selected because of its responsiveness at high Cl concentrations; a Cl-insensitive dye, Cl-NERF-dextran, was used as a reference. Both dyes were excited at 325 nm, and ratios of the fluorescence intensity at spectrally distinct emission wavelengths were obtained from two intensified CCD cameras, one for ABQ-dextran the other for Cl-NERF-dextran. LIS Cl concentration was calibrated *in situ* by treating the monolayer with digitonin or ouabain and varying the perfusate Cl between 0 and 137 mM (HEPES buffer) or between 0 and 127 mM (bicarbonate/CO_2 buffer). LIS Cl in HEPES-buffered solutions averaged 176 ± 19 mM (n = 12), calibrated with digitonin, and 170 ± 9 mM (n = 12), calibrated with ouabain. LIS Cl in bicarbonate/CO_2-buffered solutions averaged 174 ± 10 mM (n = 7) using the ouabain calibration. The Cl concentration of MDCK cell domes, measured with Cl-sensitive microelectrodes and by microspectrofluorimetry, did not differ significantly. Images of the LIS at 3 focal planes, near the tight junction, midway and basal, failed to reveal any gradients in Cl concentration along the LIS. LIS Cl changed rapidly in response to perfusate Cl with characteristic times of 0.8 ± 0.1 min (n = 21) for Cl decrease and 0.3 ± 0.04 min (n = 21) for Cl increase. In conclusion, (i) Cl concentration is higher in the LIS than in the bathing medium, (ii) no gradients of Cl along the depth of LIS are detectable, (iii) junctional Cl permeability is high.

Key words: Epithelia — Fluid transport — Cl transport — ABQ — Fluorescence microscopy

Introduction

Despite many morphological studies of the lateral intercellular spaces (LIS) of fluid transporting epithelia, there have only been a few attempts at direct measurement of the Cl composition of the fluid in the LIS. Gupta and Hall (1979) analyzed the fluid in the LIS of frozen, hydrated intestinal epithelium of rabbit by x-ray microprobe. They concluded that the LIS contained a solution with about 40 mM higher NaCl concentration than that of the bathing solutions. Uncertainty about these results stemmed from the fact that x-ray probe analysis of the LIS required very high spatial resolution as well as immobilization of ions during and after the freezing process. Insertion of ion-sensitive microelectrodes into the LIS of *Necturus* gallbladder showed that the ionic activities of Na, K and Cl exceeded those in the bathing solution by ~7 mM (Curci & Frömter, 1979; Simon et al., 1981). These investigators pointed out that their estimates of LIS ionic composition were subject to errors arising from electrode tip potentials as well as from disturbances in LIS geometry and fluid flow patterns. Furthermore, these studies did not address a key component of the standing-gradient hypothesis of Diamond and Bossert (1967)—the presence of a gradient in osmolarity

* *Present address:* Department of Urology, Akademiska sjukhuset, S 75185 Uppsala, Sweden

Correspondence to: P. Xia

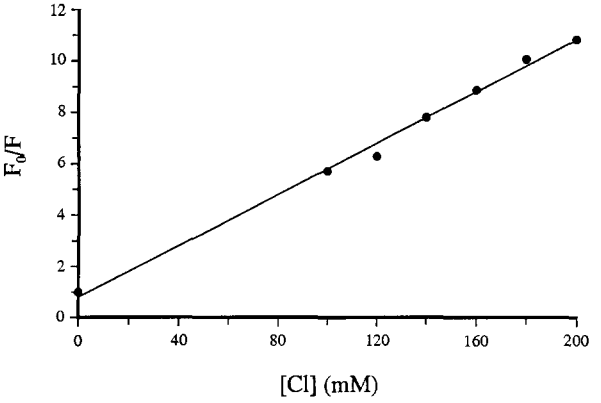

Fig. 1. Stern-Volmer plot for fluorescence quenching of ABQ-dextran measured with a spectrofluorimeter. F_0/F is the fluorescence in the absence of Cl divided by fluorescence in the presence of Cl.

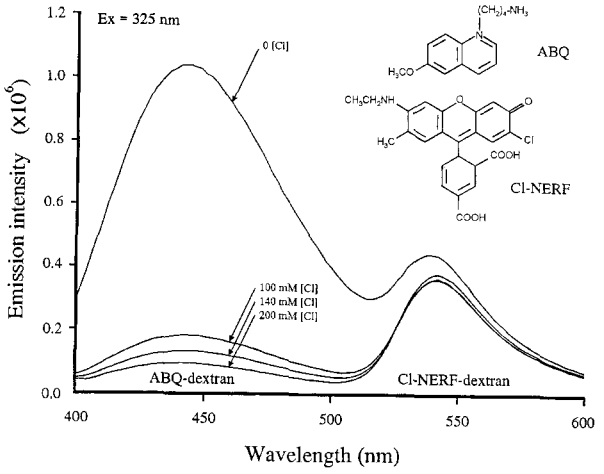

Fig. 2. Fluorescence emission spectra for a mixture of ABQ-dextran and Cl-NERF-dextran at various concentrations of Cl measured in a spectrofluorimeter. The Cl-NERF-dextran emission intensity is distorted by the crossover from the ABQ-dextran signal at low Cl concentrations.

along the depth of the LIS from tight junction to basal opening.

Because of the small size and inaccessibility of the LIS, optical microscopic spectrofluorimetry seemed an ideal method for determination of LIS Cl concentration. Recently, LIS pH has been measured by video microspectrofluorimetry of the cultured renal epithelial cell line MDCK in cells grown on glass coverslips (Harris et al., 1994) or on permeable supports (Chatton & Spring, 1994). In the present study, quantitative light microscopic methods were developed to measure the LIS Cl concentration in MDCK cells grown on glass coverslips as well as to determine the permeability of the tight junction to Cl.

Materials and Methods

Cell Culture

Madin-Darby canine kidney (MDCK) cells, passage number 65–78 (American Type Culture Collection, Rockville, Maryland), were grown on 25 mm diameter round glass coverslips and incubated at 37°C temperature with 5% CO_2/95% air. Cells were fed every other day with Dulbecco's modified Eagle's medium containing 10% fetal bovine serum and 2 mM glutamine. The medium did not contain riboflavin, phenol red, or antibiotics. Cells were used for experiments about 5 to 10 days after seeding at which time they reached confluence and made many fluid-filled domes.

Perfusion System and Perfusion Solutions

The apical surface of the monolayer was perfused with *N*-2-hydroxyethylpiperazine-*N'*-2-ethanesulfonic acid (HEPES) or bicarbonate-buffered Ringer solutions, with or without chloride. All the solutions contained (in mM) 142 Na, 5.3 K, 1.8 Ca, 0.8 Mg, 0.8 SO_4, and 5.6 D-glucose. The HEPES buffer contained 14 HEPES and 137 mM Cl. The bicarbonate/CO_2 buffer contained 24 HCO_3 and 127 mM Cl. The 0-Cl solutions contained 5.3 acetate, 3.6 lactate, and 128 NO_3 for HEPES buffer or 118 NO_3 for bicarbonate/CO_2 buffer. HEPES solutions were adjusted to pH value of 7.6 at room temperature. The solutions were delivered from water-jacketed, temperature-controlled reservoirs (at 37°C) and gassed with room air (HEPES solutions) or 7% CO_2/93% air (bicarbonate solutions). The effluent pH value was 7.4 for all solutions; perfusion rate was controlled by hydrostatic pressure regulated by compression of the tubing. The perfusion solution was switched rapidly by computer-controlled pinch valves.

Chemicals

Digitonin and ouabain octahydrate were purchased from Sigma Chemical (St. Louis, MO). Bovine albumin (fraction V) was from Miles (Kankakee, IL). All dyes were obtained from Molecular Probes (Eugene, OR).

Dye Characterization

Several Cl-sensitive fluorescent indicators, including 6-methoxy-*N*-(sulfopropyl) quinolinium (SPQ), 6-methoxy-*N*-ethylquinolinium chloride (MEQ), phenylquinoline-lucifer yellow dextran (PQLYD), and 6-methoxy-*N*-(4-aminoalkyl)quinolinium bromide hydrochloride (ABQ) (Biwersi et al., 1992) were tested. The Cl-sensitive fluorescent indicator, ABQ, and the Cl-insensitive reference dye, Cl-NERF, were both conjugated to dextrans (MW 10,000). The molar labeling ratios were 3.7 ABQ molecules/dextran and ~2 Cl-NERF molecules/dextran respectively. The spectral properties and Cl sensitivities of all of these dyes were investigated on a fluorescence spectrometer (FluoroMax, Spex Industries, Edison, NJ). In these experiments, the dyes were dissolved in solutions buffered with HEPES, and NaCl was added to the 0.5 ml cuvette from concentrated solutions (1 or 4 M.)

ABQ-dextran was selected as the Cl indicator of choice because it showed a linear and large quenching response to Cl from 0 mM to 200 mM (Fig. 1). ABQ-dextran has a peak excitation wavelength at 320 nm and a single peak emission wavelength at 444 nm, without an isosbestic point (Fig. 2). Since it has been reported that the quinolinium dyes exhibit a reduction in the Stern-Volmer slope for Cl in cellular envi-

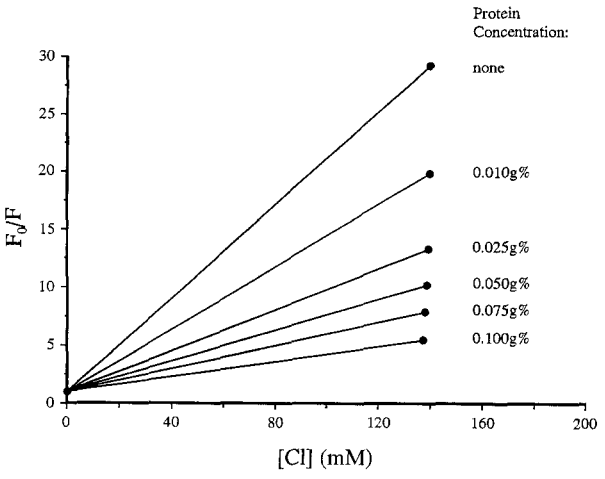

Fig. 3. Protein effects on the Stern-Volmer coefficient for fluorescence quenching of ABQ-dextran measured in a spectrofluorimeter. F_0/F is the fluorescence in the absence of Cl divided by fluorescence in the presence of Cl. The amount of albumin added to the cuvette is shown in g%.

ronments compared to free solution (Krapf, Berry & Verkman, 1988), we were concerned that protein in the LIS might exert a similar effect. When albumin was added to the Ringer solutions in the spectrofluorimeter cuvette, quenching by Cl diminished (Fig. 3). The magnitude of the protein effect led us to conclude that the ABQ-dextran calibration must be done *in situ*, not in the cuvette or capillary. The Stern-Volmer coefficient of ABQ-dextran was insensitive to changes in solution pH ranging from 6.5 to 8.5. The presence of digitonin (from 1 to 10 μM) reduced the emission intensity, however, it did not change the Stern-Volmer coefficient.

The reference dye, Cl-NERF, conjugated to a dextran with the same molecular weight as that of ABQ-dextran's, was mixed with the ABQ-dextran. Attempts to attach both probes to the same dextran molecule were unsuccessful because of inconsistent molar labeling ratios. Although Cl-NERF is normally excited at 514 or 488 nm, it also shows fluorescence when excited at 325 nm. The emission peaks for ABQ-dextran and Cl-NERF-dextran were at 444 nm and 542 nm, respectively. Figure 2 shows that although Cl-NERF-dextran does not respond to Cl concentration changes, crossover emission from ABQ-dextran distorts the Cl-NERF-dextran emission spectrum at 0 or low Cl concentrations. A crossover magnitude of 26 ± 1.5% was determined in the LIS by loading ABQ-dextran alone and measuring the fluorescence intensity at different Cl concentrations from both the ABQ-dextran and Cl-NERF-dextran channels.

Fluorescence Microscopy Setup

Figure 4 shows an overview of the optical and electronic system. The fluorescence excitation light source was a single wavelength 21 mW He-Cd laser (Model 3056-15, Omnichrome, Chino, CA). The 325 nm output beam was coupled to the microscope through lens L1, shutter S1 and a multimode single fiber wave guide. Beam intensity was controlled with a quartz neutral density step wedge (ND1, Reynard Optics, Laguna Nigel, CA). Vibrating the fiber, by wrapping it around the cooling fan of the laser head, assured phase randomization of the light beam, as attested to by the disappearance of the speckle due to the coherence of laser light (Chatton & Spring, 1993). Fluorescence measurements were made on an inverted microscope (Diaphot, Nikon Microscope Inc., Melville, NY) with a Nikon Fluor oil immersion objective (100×, numerical aperture 1.30, 250 μm working distance). The UV excitation beam was reflected to the specimen by a 400 nm dichroic mirror (DM1, Omega Optical, Brattleboro, VT). The fluorescence emissions from the two dyes were collected by the objective, and transmitted through the dichroic mirror to a multi-image module (Nikon) for detection. The longer wavelength emission passed through a 505 nm dichroic mirror (DM2, Omega) and a 520 nm long-pass filter (F2, Omega) to an image intensifier I1 (KS-1381, Videoscope, Washington, DC), coupled to CCD camera CCD1 (CCD-72, Dage MTI, Michigan City, IN). The shorter wavelength emission was reflected by the 505 nm dichroic mirror (DM2) to image intensifier I2 (KS-1381, Videoscope), coupled to a second CCD camera CCD2 (200E, Videoscope).

Transmitted light was used to visualize the monolayer for focusing and dye loading. The transmitted light path included a tungsten lamp, shutter (S2), neutral density filter (ND2), long wavelength (600 nm) filter (F1) and a Leitz long-working distance condenser-objective (32×, numerical aperture 0.4). The transmitted light shutter (S2) was opened only when fluorescence excitation was shuttered off. The transmitted light image passed through the two dichroic mirrors and the filter F2 and appeared in the Cl-NERF-dextran channel. Accurate focusing and optical sections of known thickness were obtained by stepper motor-driven displacement of the specimen stage.

Image Acquisition and Data Analysis

Video images from the CCD cameras were digitized at 8-bits by an image acquisition system (Image-1/AT, Universal Imaging, West Chester, PA) interfaced to an IBM 386 computer. To ensure that fluorescence was measured in the same region of the LIS, images in the two channels were registered by adjustment of a mirror in the multi-image module. A pair of images were acquired from the two channels for each data point. A 32-frame exponential running average was applied to each image for noise reduction. The intensifier percentage gain for each image was controlled by the computer and automatically recorded in a log file during the experiment. Several steps were required to obtain the absolute intensity value of fluorescence. (i) A region in which the intensity was relatively uniform along the LIS and in which the geometrical shape of LIS was well maintained throughout the whole experiment was selected. The registration and uniformity of a pair of images was estimated at the beginning of the whole experiment by obtaining a false-color ratio image of ABQ-dextran and Cl-NERF-dextran at the same time point and focal plane (Fig. 5). (ii) A binary image mask representing segmentation of the bright LIS area and the dark cells was generated by thresholding the gray level of the Cl-NERF-dextran image to define the measurement region of interest. This binary mask was then applied to the corresponding ABQ-dextran image to define the same LIS region of interest. The mean intensity within the area bounded by the mask for each image was calculated. (iii) These mean intensities were normalized by the corresponding intensifier absolute gain. (iv) As described in the *Dye Characterization*, crossover corrections were applied to every pair of images.

Dye Loading

Coverglasses with MDCK monolayers were mounted in an open perfusion chamber (40 μl volume) on the stage of the microscope. A sharpened micropipette, tip diameter about 5 μm, was mounted on a precision 3-D translation stage and connected to a microinjector (model 5242, Eppendorf, Madison, WI). The perfusion chamber was temperature-controlled at 37°C with peltier elements. The operating parts of the microscope and the specimen stage were enclosed in a light-tight

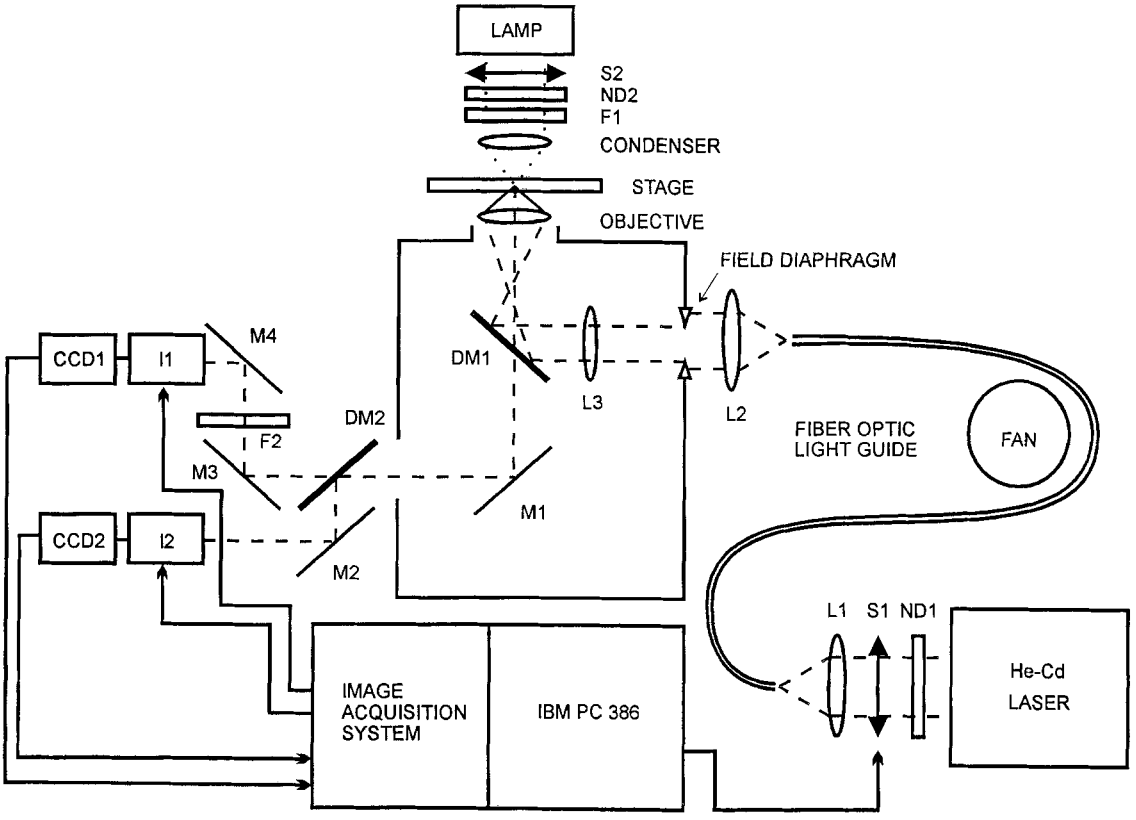

Fig. 4. Diagram of the experimental setup. Abbreviations are as follows: *ND,* neutral-density filter; *S,* shutter; *L,* lens; *DM,* dichroic mirror; *M,* mirror; *F,* filter; *I,* image intensifier. The different components are described in detail in the text. The dotted lines represent the bright field illumination light path; the dashed lines are the paths of laser light illumination and fluorescence emission.

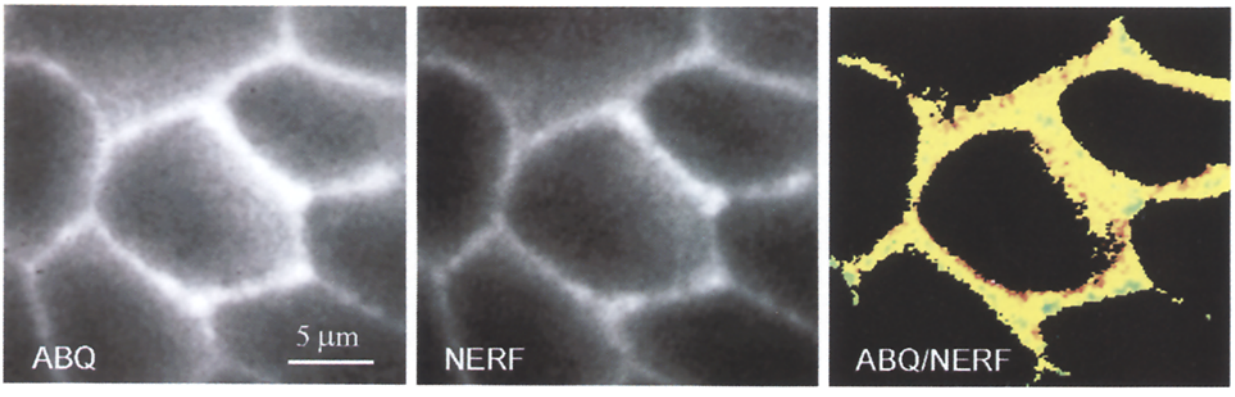

Fig. 5. Typical images (32-frame average) of MDCK LIS loaded with ABQ-dextran and Cl-NERF-dextran. The ABQ-dextran image was captured by CCD2 which collected the emission from 400 to 505 nm; the Cl-NERF-dextran image was captured by CCD1 which collected the emissions longer than 530 nm. The ABQ-dextran/Cl-NERF-dextran ratio image was obtained by dividing these two images pixel by pixel. The entire range of colors shown correspond to a variation of the ratio of less than 10%.

box whose temperature was maintained at 30°C by an air circulating system. After the monolayer was perfused for about 10 min, a mixture of 20 mM ABQ-dextran and 10 mM Cl-NERF-dextran in Cl-free HEPES-buffered solution was loaded into the micropipette tip. A dome was punctured and a small volume of solution (typically less than 10% of the dome volume) was injected by an air pressure pulse. Images were normally taken 5 min after dye injection in an area two-to-three cells away from the edge of the injected dome. Diffusion of both dyes away from the dome and into the LIS occurred at a similar rate as determined from their respective concentration profiles. Both dyes have approximately the same diffusion coefficient in the extracellular space, $14 \pm 1 \times 10^{-7}$ cm^2 s^{-1} (Nicholson & Tao, 1993).

Ion-sensitive Microelectrode Measurements

Cl-sensitive and 3 M KCl-filled, voltage-sensitive microelectrodes were fabricated as previously described (Fisher & Spring, 1984). The electrodes were connected to a high impedance amplifier (model FD-223, World Precision, Sarasota, FL) whose output was recorded by a computerized data acquisition system (Fisher & Spring, 1984). The reference electrode was a calomel cell immersed in 3 M KCl and connected to the apical bath by a HEPES-buffer filled agar bridge. Acceptable Cl-sensitive electrodes had a mean slope of 56.7 ± 0.3 mV/decade (calibrated in NaCl standards). Criteria for a measurement of Cl activity in MDCK cell domes included a stable, accurate value for Cl activity in the perfusate before and after a measurement in the dome. Voltage-sensitive electrode measurements were accepted only when the readings in the apical bath before and after puncture of the dome agreed to within 1 mV and input resistance was unchanged.

Statistics

All data are presented as mean ± SEM. The Student's *t*-test was used to determine significance of differences.

Results

Dye Loading and In Situ Calibration

The steady-state ABQ-dextran concentration in the LIS two-to-three cell diameters away from the dome was ~100 μM, estimated from the absolute intensity. ABQ-dextran fluorescence was calibrated *in situ* as a function of LIS Cl concentration by perfusing Cl-free or control perfusion solutions in conjunction with digitonin or ouabain treatment of the monolayer. The Stern-Volmer coefficient and the unknown Cl concentration inside the LIS were then determined. The average Stern-Volmer constant for Cl in the LIS was 15 ± 3 M^{-1} (n = 31) for MDCK cells.

Two strategies for *in situ* calibration were employed to ensure that LIS Cl concentration varied in synchrony with perfusate Cl. In the first method, the monolayer was permeabilized by digitonin; the optimum concentration for digitonin was found to be 2.5 μM with an exposure time of about 2 min. The second strategy was to block NaCl transport by perfusing the monolayers with ouabain and wait until LIS Cl reach a new steady state, presumably equal to that of the perfusion solution. The optimum concentration for ouabain was found to be 0.1 mM with equilibration occurring in about 5 min.

LIS Chloride Concentration in HEPES-buffered Solutions

After the MDCK cells were mounted in the chamber and perfused with 137 mM Cl HEPES-buffered solution for about 10 min, a mixture of ABQ-dextran and Cl-NERF-dextran dyes in Cl-free HEPES buffer was injected into a dome, allowing to diffuse for 5 to 10 min and then image acquisition was started at the LIS near the dome. One pair of images was acquired every minute throughout the whole experiment. To avoid photobleaching, the UV excitation shutter (S1) was opened only for the approximately 5 sec required for acquisition of the image pair. A minimum of three data points were obtained for the unknown Cl concentration in LIS, then the perfusate was switched to a solution of the same composition containing digitonin. After 5 min of digitonin permeabilization, five pairs of images were acquired. Then the perfusate was switched to Cl-free HEPES-buffered solution containing digitonin for at least another 5 min.

The experimental procedure for ouabain calibration was similar to that of the digitonin calibration. Since the ouabain treatment took longer than the digitonin permeabilization, a pair of images was acquired every 2 min throughout the experiment. The time required for perfusion with 137 mM Cl or zero Cl HEPES-buffered solutions was 15 min or longer, so at least seven pairs of images were taken in each condition.

A typical experiment is shown in Fig. 6. The ratio of ABQ-dextran/Cl-NERF-dextran in the three different perfusates is shown in *B:* the unknown Cl concentration, 137 mM Cl plus ouabain, and Cl-free plus ouabain. Steady-state values of the respective ratios were determined by inspection. Signals from both fluorophores exhibited an exponential decline as a function of time, presumably because of diffusion of the dyes into adjacent LIS as well as photobleaching of the dyes in the field of view. The Stern-Volmer slope was obtained from the two-point *in situ* calibration and the unknown Cl concentration was then calculated. The LIS Cl concentration in HEPES-buffered solutions was 176 ± 19 mM (n = 12), calibrated with digitonin and 170 ± 9 mM (n = 12), calibrated with ouabain.

LIS Chloride Concentration in Bicarbonate-buffered Solutions

Ouabain inhibition was also used as a calibration procedure for the studies of monolayers perfused with bicarbonate/CO_2 buffered solutions. The Cl concentration in the perfusate was 127 mM and the HCO_3 concentration was 24 mM. Despite the lower Cl concentration of the perfusate, LIS Cl averaged 174 ± 10 mM (n = 7), not significantly different from that observed in the HEPES-buffered solutions. Figure 7 compares the LIS Cl during perfusion with HEPES or bicarbonate-buffered solutions.

Chloride Concentration in Domes

The Cl activity in the HEPES-buffered perfusate, measured by Cl-sensitive microelectrodes was 110 ± 0.9 mM, corresponding to a concentration of 141.6 ± 1.1 mM (n =

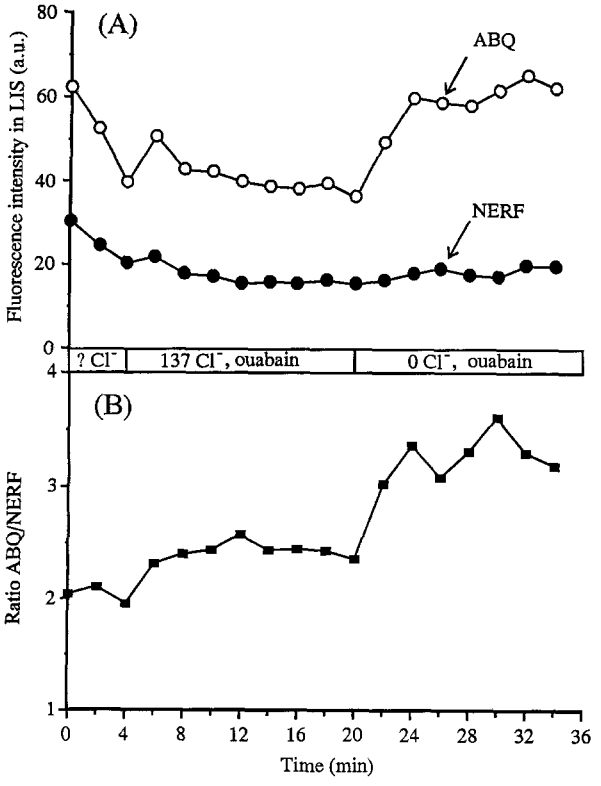

Fig. 6. Typical experimental result showing an *in situ* calibration procedure. (*A*) shows the fluorescence intensity (arbitrary units) in a selected region of LIS measured from ABQ-dextran channel and Cl-NERF-dextran channel. Zero time on the abscissa represents 5 to 10 min after the dye loading. The monolayer was perfused with HEPES-buffered 137 mM Cl Ringer. At 4 min, the perfusate was switched to a solution of the same composition with 0.1 mM ouabain added and at 20 min, the perfusate was switched to a Cl-free solution with ouabain. The data points were normalized for the absolute gain of intensifiers and corrected for crossover. (*B*) shows the corresponding ratio of the fluorescence of ABQ-dextran to Cl-NERF-dextran; higher ratios correspond to lower Cl concentrations. Note that the parallel decrease in both the ABQ and Cl-NERF signals in *A* is compensated for by use of the ratio.

45). This value differs significantly from a Cl concentration of 137 mM, determined chemically. The difference presumably stems from interference by anions other than Cl in the perfusion solution. The Cl activity measured in the dome fluid was 108.9 ± 0.8 mM, corresponding to a concentration of 140.2 ± 1.0 mM (n = 45). Neither the activity nor the calculated Cl concentration in the dome differed significantly from that measured in the perfusate. The transepithelial potential difference was −1.83 ± 0.27 mV (n = 8), dome interior negative to the apical perfusate.

Measurement of dome Cl by microspectrofluorimetry employed calibration solutions in capillaries rather than *in situ* calibration because of the relatively large

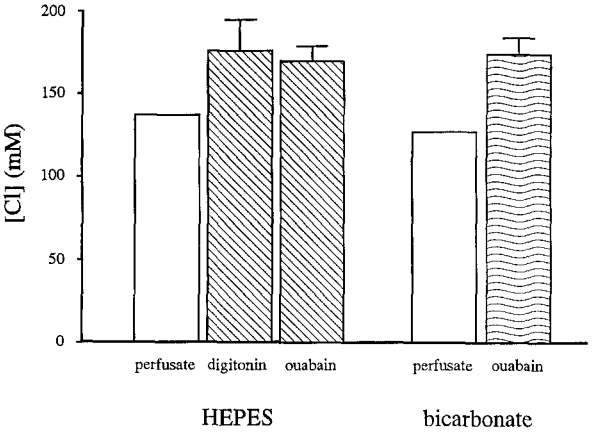

Fig. 7. Mean Cl concentration of LIS in HEPES and bicarbonate/CO_2 solutions. Open bars are the perfusate Cl concentrations, 137 mM for HEPES solutions and 127 mM for bicarbonate/CO_2 solutions. The number of digitonin experiments was 12, ouabain in HEPES was 12, and ouabain in bicarbonate/CO_2 was 7.

fluid volume of the domes (typical dome volumes ranged from 10 to 500 pl) compared to that of the LIS (estimated volume 28 fl). Dome Cl concentration was 147.8 ± 13.9 mM (n = 15), not significantly different from that measured with Cl-sensitive microelectrodes or chemically in the perfusate.

Chloride Concentration along the LIS

The Cl concentration along the apical-to-basal LIS axis was also investigated. Optical sections were obtained at three locations along the LIS separated from each other by 2.4 μm steps: the basal surface adjacent to the coverglass, middle, and apical region adjacent to the tight junction. The height of the LIS of MDCK cells was around 6 ± 1 μm at the time of the experiments. Figure 8 shows pairs of ABQ-dextran and Cl-NERF-dextran images (32-frame average) at these three different optical sections. The experimental procedure was the same as described above: the monolayers were perfused with HEPES-buffered solution, the Stern-Volmer slope was calibrated *in situ* at each focal plane by adding ouabain to the solution and subsequently switching the Cl concentration from 137 mM to 0 mM. Three pairs of images were acquired for each time point. The mean values of Cl concentration at the three focal planes did not differ significantly nor was there any detectable gradient in Cl along the LIS (Fig. 9).

Transients in LIS Chloride

Experiments were done to evaluate the rate of Cl change in LIS when the perfusate Cl concentration of HEPES-

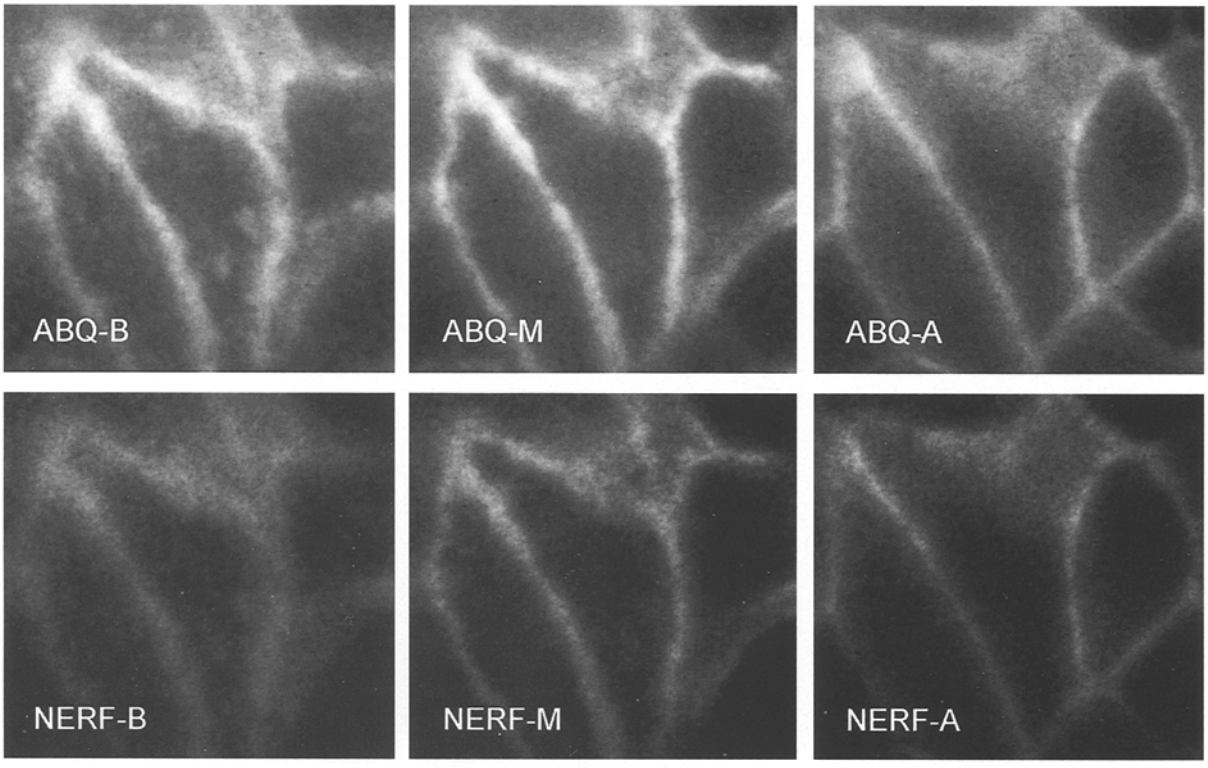

Fig. 8. Images for ABQ-dextran and Cl-NERF-dextran taken at three optical sections of MDCK LIS, where *B* is basal surface, *M* is the middle section, and *A* is apical section. The distance between each section was 2.4 μm.

buffered solutions was rapidly switched between 137 mM and 0 mM. The perfusion rate for this experiment was adjusted to 28 μl/sec so that the 40 μl chamber volume was replaced every 1.5 sec. To achieve rapid imaging, only ABQ-dextran images were acquired at 5-sec intervals. The excitation light source was shuttered off between images to minimize photobleaching. Figure 10 shows an example of the experimental results and curve fitting. (*A*) shows the transient response of the ABQ-dextran fluorescence intensity to the perfusate Cl concentration change. This curve was corrected by subtracting the background signal due to dye leakage and the data were fitted using the Levenberg-Marquardt algorithm by the equation:

$$I = a_1 + a_2 \exp\left(-\frac{t}{\tau}\right)$$

where I is the fluorescence intensity, t is the time, τ is the characteristic time constant, a_1 and a_2 are the optimized parameters. (*B*) and (*C*) are examples of the curve fit for a fluorescence intensity increase (decreasing Cl) and decrease (increasing Cl), respectively.

The characteristic times from 21 experiments are shown in Fig. 11. The LIS Cl changed rapidly in re-

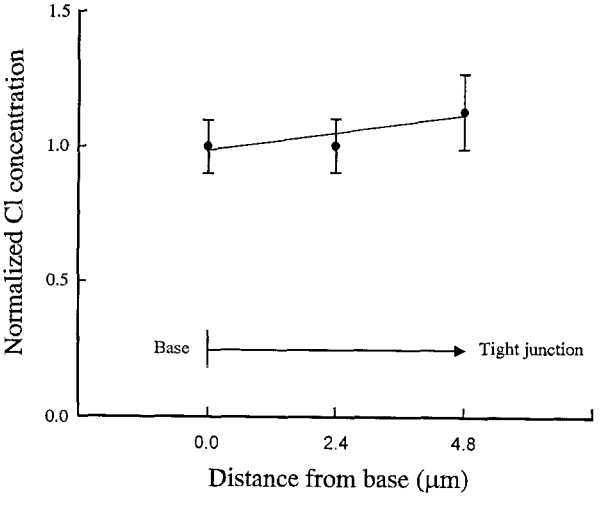

Fig. 9. Cl concentration along the LIS of MDCK cells perfused with HEPES-buffered solutions. The values were normalized to the Cl concentration at the basal surface of LIS. The solid line, drawn by the method of least squares, has a slope of 0.027 ± 0.033, not significantly different from 0. The correlation coefficient for the line was 0.17, indicative of the lack of correlation between Cl concentration and depth of the LIS.

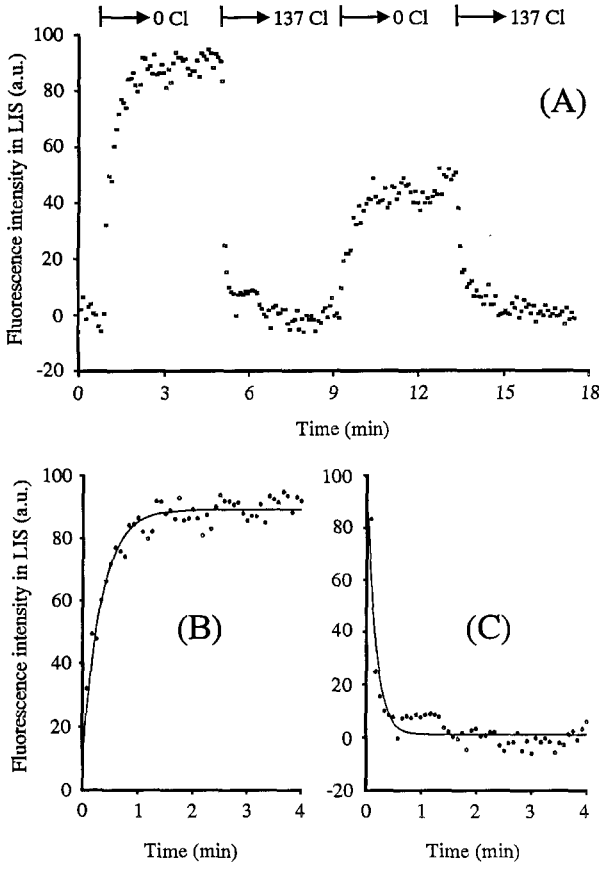

Fig. 10. Transient response of Cl concentration in the MDCK LIS to the perfusate Cl changes. (*A*) is the experimental record. (*B*) and (*C*) are examples of nonlinear curve fitting.

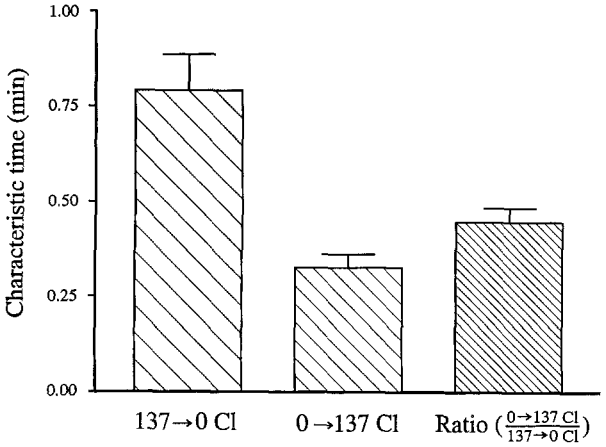

Fig. 11. Mean values of characteristic times for Cl change in the LIS in response to the perfusate Cl changes. The number of experiments was 21.

sponse to perfusate Cl with characteristic times of 0.8 ± 0.1 min ($n = 21$) for Cl decrease and 0.3 ± 0.04 min ($n = 21$) for Cl increase. This result is consistent with the conclusion that junctional Cl permeability is relatively high.

Discussion

The present results constitute the first direct measurements of the Cl concentration of the LIS of mammalian cells. Several points are worthy of note: (i) LIS Cl concentration was consistently higher than perfusate Cl, (ii) the presence of HCO_3 had little effect on LIS Cl, (iii) no gradients in Cl along the depth of the LIS were detectable, (iv) tight junctional Cl permeability was high, (v) the Cl concentration in large domes was indistinguishable from the bathing medium both by microelectrode and microspectrofluorimetric methods. Of central concern is the validity of the methods used for calibration and calculation of the Cl concentration in the LIS as well as the relevance of observations in MDCK cells to others fluid-transporting epithelia.

Dye Selection, Calibrations and Sources of Error

The quinolinium dyes represent the only current practical group of fluorescent indicator dyes for Cl and other anions. They are cationic dyes whose fluorescence is quenched by collision with selected anions (Urbano, Offenbacher & Wolfbeis, 1984). Because these dyes do not exhibit spectral shifts or isosbestic points that would make ratio measurements possible, it has been difficult to ensure that the decreases in fluorescence observed are due to quenching by the anion of interest rather than to nonspecific effects. Indeed, the earliest report on the quinolinium dyes described a reduction in the Stern-Volmer relationships as a result of dye immobilization in a polymer layer (Urbano et al., 1984). The most commonly used quinolinium indicator, SPQ, exhibits an approximately tenfold reduction in its Stern-Volmer slope for Cl in cells compared to free solution (Krapf et al., 1988). Although this effect was initially postulated to be a consequence of the putative high viscosity of cytoplasm (Krapf et al., 1988), it has subsequently been convincingly demonstrated that cytoplasmic viscosity is not very different from that of water (Kao, Abney & Verkman, 1993; Luby-Phelps et al., 1993) and that the fluorescence lifetime of SPQ changes in a manner consistent with partial immobilization of the dye by intracellular proteins (Krapf et al., 1988). In the present study the sensitivity of the quinolinium dyes to Cl was profoundly diminished by the presence of proteins in relatively low concentration as clearly demonstrated in calibrations carried out in a spectrofluorimeter. In a previous study, MDCK cell LIS pH was acidic compared to the bathing

solution and was not sensitive to inhibitors of acid-base transport or temperature reduction (Chatton & Spring, 1994). The stability of LIS pH and the relative acidity of the LIS were attributed to the microenvironment created by negatively charged cell surface proteins. Thus, the previous studies showed that the LIS environment was strongly influenced by proteins on the adjacent basolateral cell membranes as well as by any soluble proteins within the LIS.

The strategies employed in the present study to cope with the protein effects and limitations of the fluorescent probes was the use of a mixture of two spectrally distinct dyes attached to high molecular weight dextrans combined with *in situ* calibration by two different methods. ABQ-dextran was selected as the Cl indicator for the present experiments because it exhibited, in the spectrofluorimeter, an appropriate Stern-Volmer coefficient for quenching by the Cl concentration expected in the LIS. Because the reference dye, Cl-NERF-dextran, is negatively charged, it was not significantly influenced by added proteins either in the cuvette or in glass capillaries.

Our requirements for an acceptable *in situ* calibration included constancy of LIS width during Cl replacement with NO_3, uniformity of ratio over the area of interest, stability of the ratio after permeabilization by digitonin or transport inhibition by ouabain, a Stern-Volmer coefficient of 6 or greater, signal-to-noise ratio of 5 or greater. A combination of the above criteria and the similarity of LIS Cl concentration calibrated by two methods—digitonin or ouabain treatment in HEPES or bicarbonate buffered solution—gives us greater confidence in the absolute values obtained. Of concern in the calibrations was the assumption that LIS Cl equilibrated completely with that of the perfusate after ouabain or digitonin treatment. Incomplete equilibration would result in an artifactually low Stern-Volmer coefficient and an overestimate of LIS Cl concentration. This possibility was evaluated by plotting the LIS Cl concentration versus the Stern-Volmer coefficient for each determination. There was no relationship between the magnitude of the Stern-Volmer coefficient in an individual LIS and the Cl concentration of that LIS.

Ion-sensitive microelectrode studies of the domes served as additional controls on the microspectrofluorimetry and showed that the Cl activity within larger domes did not differ significantly from that in the bathing medium. The apparent Cl concentration within the dome that was determined with fluorescent dyes, agreed reasonably well with the microelectrode measurements. The dome Cl concentration calculated from the fluorescent dyes was 147.8 mM, about 10 mM higher than the chemically determined Cl concentration of the perfusate (137 mM). Because of the relatively large standard error associated with the microspectrofluorimetric measurements, we can not rule out the possibility that the Cl concentrations measured by the fluorescent dyes exhibit a systematic bias of about 10 mM toward higher values than those measured chemically.

LIS Cl Physiological Significance

The measured LIS Cl concentration was consistently about 30 mM greater than that of the bathing medium in both the presence and absence of HCO_3. Because of the above-mentioned systematic errors associated with the measurement of Cl by microspectrofluorimetry, the difference between LIS and perfusate Cl could be as small as 20 mM. In agreement with this estimate, another study (Chatton & Spring, 1995) showed that the LIS Na concentration of MDCK cells exceeded that of the apical perfusate by ~15 mM in the presence of bicarbonate. A 20 mM NaCl concentration gradient between LIS and apical perfusate would lead to a predicted LIS osmolality about 40 mOsm/kg H_2O higher than that of the apical bath. Two consequences of a gradient in salt concentration and osmolality between LIS and apical bath are back diffusion of NaCl from LIS to apical bath and water flow from the apical bath to the LIS across both the tight junction and cellular membranes. Maintenance of an elevated NaCl concentration in the LIS requires that the water permeability of the cell membranes be relatively modest. Inhibition of Na transport by ouabain or permeabilization by digitonin caused LIS Cl concentration indicated by the ratio measurements to fall, consistent with the conclusion that LIS Cl always exceeded bathing solution Cl concentration. Since the transient response experiments showed that the Cl conductance of the tight junction was high, the elevated LIS Cl must be due to transport. The Cl extrusion rate required to maintain this concentration gradient can be estimated from the measured tight junctional permeability properties and LIS Cl concentration.

A typical MDCK cell, with a volume of 480 fl and an intracellular Cl concentration of 60 mM (Macias et al., 1992), has a Cl content of about 29 fm. An estimated LIS volume of 28 fl and measured LIS Cl of 170–175 mM leads to a calculated LIS Cl content of 4.7 fm. From the transient measurements of a half-time for Cl efflux of 0.8 min, the transjunctional Cl flux with a zero-Cl perfusate is 3.8 fm/min. For the transjunctional driving force of 20–30 mM existing during perfusion of 137 mM Cl, the calculated Cl efflux would be about 0.7 fm/min. Thus about 15% of the LIS Cl content would be lost each minute as a result of diffusion across the tight junction. This Cl must be replaced by transport from the cell to the LIS. Such a Cl flux represents only about 2% of the intracellular Cl content and, therefore, constitutes only a minor fraction of the transepithelial transport for a typical epithelial cell. The maximum rate of transcellular Cl

transport can be estimated from the characteristic time of 0.3 min for refilling the LIS with Cl (Fig. 9). The Cl flux into the LIS based on this time constant would be 10 fm/min, about 6.2 fm/min larger than the efflux across the tight junction estimated above. A transport rate of 6.2 fm/min across the basolateral membrane into the LIS is consistent with complete turnover of all intracellular Cl in about 5 min.

Since the Cl concentration in the domes was also 20–30 mM less than in the LIS, a gradient in Cl concentration should exist within the LIS adjacent to a dome. Our efforts to detect and analyze this putative gradient were frustrated by the overriding effects of the protein concentration differences between LIS and domes.

Finally, the rate of change of Cl within the LIS was much faster than that reported for Na in a recent publication from this laboratory (Chatton & Spring, 1995). This was unexpected as previous investigators have reported that MDCK tight junctions are cation selective with a t_{Na} of about 0.64 (Oberleithner et al., 1990). Our interpretation of these results, at this time, is that the rate of Cl efflux is representative of tight junctional permeability properties, while the Na transients significantly underestimate the junctional Na permeability. Further studies of this subject are presently under way.

In summary, LIS Cl was higher than that of the perfusate by 20–30 mM, no gradients in Cl concentration could be detected along the depth of the LIS, junctional Cl permeability was relatively high, and the elevated LIS Cl concentration could be maintained by a very modest rate of transport from the cell to the LIS.

We gratefully acknowledge the assistance of Mr. Richard D'Alessandro in the performance of the microelectrode studies. Mr. Carter Gibson designed the electronics and wrote the key computer programs used in this study. The authors are grateful to Dr. Alan Verkman (UCSF) for his advice and gifts of fluorescent probes in the early stages of this work.

References

Biwersi, J., Farah, N., Wang, Y.-X., Ketcham, R., Verkman, A.S. 1992. Synthesis of cell-impermeable Cl-sensitive fluorescent indicators with improved sensitivity and optical properties. *Am. J. Physiol.* **262:**C243–250

Chatton, J.-Y., Spring, K.R. 1993. Light sources and wavelength selection for widefield fluorescence microscopy. *MSA Bull.* **23:**324–333

Chatton, J.-Y., Spring, K.R. 1994. Acidic pH of the lateral intercellular spaces of MDCK cells cultured on permeable supports. *J. Membrane Biol.* **140:**89–99

Chatton, J.-Y., Spring, K.R. 1995. The sodium concentration of the lateral intercellular spaces of MDCK cells: a microspectrofluorimetric study. *J. Membrane Biol.* **145:**11–19

Curci, S., Frömter, E. 1979. Micropuncture of lateral intercellular spaces of *Necturus* gallbladder to determine space fluid K^+ concentration. *Nature* **278:**255–257

Diamond, J.M., Bossert, W.H. 1967. Standing-gradient osmotic flow. A mechanism for coupling water and solute transport in epithelia. *J. Gen. Physiol.* **50:**2061–2083

Fisher, R.S., Spring, K.R. 1984. Intracellular activities during volume regulation by *Necturus* gallbladders. *J. Membrane Biol.* **78:**187–199

Gupta, B.L., Hall, T.A. 1979. Quantative electron probe x-ray microanalysis of electrolyte elements within epithelial tissue compartments. *Fed Proc.* **38:**144–53

Harris, P.J., Chatton, J.-Y., Tran, P.H., Bungay, P.M., Spring, K.R. 1994. Optical microscopic determination of pH, solute distribution and diffusion coefficient in the lateral intercellular spaces of epithelial cell monolayers. *Am. J. Physiol.* **266:**C73–C80

Kao, H.P., Abney, J.R., Verkman, A.S. 1993. Determinants of the translational mobility of a small solute in cell cytoplasm. *J. Cell Biol.* **120:**175–184

Krapf, R., Berry, C.A., Verkman, A.S. 1988. Estimation of intracellular chloride activity in isolated perfused rabbit proximal convoluted tubules using a fluorescent indicator. *Biophys. J.* **53:**955–962

Luby-Phelps, K., Mujumder, S., Ernst, L., Galbraith, W., Waggoner, A. 1993. A novel fluorescence ratiometric method confirms the low solvent viscosity of the cytoplasm. *Biophys. J.* **65:**236–242

Macias, W.L., McAteer, J.A., Tanner, G.A., Fritz, A.L., Armstrong, W.McD. 1992. NaCl transport by Madin-Darby canine kidney cyst epithelial cells. *Kidney Int.* **42:**308–319

Nicholson, C., Tao, L. 1993. Hindered diffusion of high molecular weight compounds in brain extracellular microenvironment measured with integrative optical imaging. *Biophys. J.* **65:**2277–2290

Oberleithner, H., Vogel, U., Kersting, U., Steigner, W. 1990. Madin-Darby canine kidney cells. II. Aldosterone stimulates Na^+/H^+ and Cl^-/HCO_3^- exchange. *Pfluegers Arch.* **416:**533–539

Simon, M., Curci, S., Gebler, B., Frömter, E. 1981. Attempts to determine the ion concentrations in the lateral intercellular spaces between the cells of *Necturus* gallbladder epithelium with microelectrodes. *In:* Water Transport Across Epithelia: Barriers, Gradients and Mechanisms. H.H. Ussing, N. Bindslev, N.A. Lassen, O. Sten-Knudsen, editors. pp. 52–64. Munksgaard, Copenhagen

Urbano, E., Offenbacher, H., Wolfbeis, O.S. 1984. Optical sensor for continuous determination of halides. *Anal. Chem.* **56:**427–429